International Journal of Control, Automation and Systems 17(2) (2019) 391-404
http://dx.doi.org/10.1007/s12555-018-0376-3
ISSN:1598-6446 eISSN:2005-4092
http://www.springer.com/12555

Analytical Design and Stability Analysis of the Universal Integral Regulator Applied in Flight Control

Yohan Díaz-Méndez*, Marcelo S. de Sousa, Guilherme Gomes, Sebastião Cunha, and Alexandre Ramos

Abstract: This paper considers the analytical design and stability analysis of an output feedback flight control problem for a rigid fighter aircraft which has a highly nonlinear dynamic. In this paper, a robust technique known as Universal Integral Regulator (UIR) has been chosen to solve the tracking problem due to the possibility to demonstrate the stability of the system and analytically compute the control parameters. The UIR is a combination of Continuous Sliding Mode Control (CSMC) and a Conditional Integrator (CI) which provides integral action only inside the boundary layer, enhancing the transient response of the system and providing an equilibrium point where the tracking error is zero. The general procedure consists firstly of rewriting the aircraft dynamics in the control-affine form, then the relative degree of the system is computed and the system is transformed to normal form. An output feedback controller using a CSMC controller is proposed, and a sliding surface considering a CI is designed. The controller parameters are designed analytically, taking into account two approaches. The first approach does not consider uncertain parameters and the second one treats a stability derivative as a parametric uncertainty. Simulations were performed in order to validate the design procedure of the control technique and to demonstrate the robustness of the UIR. Detailed step by step information about the computing of the controller parameters was done and an analytical analysis of stability was developed to demonstrate the convergence of the sliding surface, conditional integrator and tracking error dynamics.

Keywords: Aircraft, nonlinear control, sliding mode control, universal integral regulator.

1. INTRODUCTION

One of the most important requirements in flight control system design is the ability of the controller to efficiently perform a robust tracking of a desired reference signal with approximately zero error. Since the dynamic of a fighter aircraft is highly nonlinear and almost all the degrees of freedom of the system are coupled, the solution of the attitude tracking problem is difficult and challenging, and according to [1] the designed controllers must address the issues of uncertainty, nonlinearity, and complexity. A common practice for tackling this problem is to linearize the aircraft dynamics around an equilibrium point (flight condition), and find the gains, which are scheduled depending upon the flight operating condition along the flight envelope [2, 3]. Then, linear control techniques can be applied; among them, linear quadratic optimal control [4, 5], and PID [6]. However, due to parametric uncertainties, various flight conditions and high non-linearity, linear control techniques do not extract enough performance from the aircraft.

Several methods have been employed to increase the robustness of the controllers and to deal with the problems and challenges of linear controllers. These linear techniques are commonly implemented through feedback linearization (FL) and transforming the system in normal form such as in [7–10] and [11], and inverting the dynamics once the FL is made [12, 13]. One important advantage of feedback linearization is the capacity of totally or locally transforming the aircraft dynamics in an equivalent system that is easy to manage, but it still does not deal with uncertainties in the model. Throughout the past decades, control techniques based on variable structure control (VSC) such as Dynamic Inversion (DI) and sliding mode control (SMC), were performed to tackle this problem and provide more robust controller designs as in [14–17] for SMC and [18] for DI.

As demonstrated in [14], SMC requires high control activity due to the chattering phenomenon caused by the definition of a switching function *sign(·)* which represents the basic procedure of SMC [19]. According to [20], the robust nonlinear control method SMC, due to the chattering,

Manuscript received June 6, 2018; revised August 17, 2018 and September 6, 2018; accepted September 28, 2018. Recommended by Associate Editor Guangdeng Zong under the direction of Editor Hamid Reza Karimi.

Yohan Díaz-Méndez, Marcelo S. de Sousa, Guilherme Gomes and Sebastião Cunha are with the Department of Mechanical Engineering, Federal University of Itajubá, 1303 BPS Avenue, Itajubá 37500-903, Brazil (e-mails: yohan.g8@unifei.edu.br, marcelo.santiago@unifei.edu.br, guilhermefergom@unifei.edu.br, sebas@unifei.edu.br). Alexandre Ramos is with the Department of Mathematics and Computing, Federal University of Itajubá, 1303 BPS Avenue, Itajubá 37500-903, Brazil (e-mail: ramos@unifei.edu.br).
* Corresponding author.

causes poor control accuracy. This excessive and permanent oscillation can excite un-modelled, high-frequency dynamics neglected in the modeling [21] and thereby produce excessive wear in the flight control actuators, possibly leading to flutter. In order to solve the chattering problem, in [22] was proposed a dynamic integral SMC strategy showing good results, nevertheless, in the present work the function *sign(·)* was substituted by the approximate function *sat(·)* as adopted in [23], but at the expense of degrading the transient response of the system. Then, at the beginning of the past decade, a new methodology was proposed by [24] to deal with this disadvantage. This is one of the reasons for which the authors consider this control technique as having great potential for implementation in the flight control problem addressed in this work. The main feature of this new controller design was the introduction of a CI capable of enhancing the transient response of the system while keeping the tracking error at zero and provide a robust, easy to implement controller. A special case of this controller design is called the Universal Integral Regulator (UIR).

The UIR has been applied in a variety of control problems, such as: liquid level in coupled tanks [25, 26], DC to DC power converters [27], path following of marine vessels [28] and satellite launchers [29]. Some applications have been pursued in aircraft control, as in the work of [30] and [31] whose design is based upon plant linearization and uses short-period and phugoid approximations. In the work of [29], although a modified UIR is proposed, detailed information about the design of the classical UIR and controller gain estimation is not provided. In the works of [32] and [33] the controller gain and boundary layer values were obtained through a trial and error process, and in [3] and [30], the UIR controller gain was assumed as the maximum allowed deflection of the control surface. That lack of information about the analytical controller gain computation motivated and encouraged the authors of this paper to show, in the present work, how these parameters are determined and applied to a control problem that had not been solved before using the theoretical design of the UIR technique. The main contributions of this work compared with earlier ones are: *i)* the nonlinear dynamics are not linearized; the highly nonlinear equations of motion are extended and rearranged in the control affine in the input form; *ii)* the maximum gain of the controller is computed and not assumed as the maximum deflection of the control surface; *iii)* the detailed information about the analytical procedure of computing the controller gain, the stability demonstration of internal and external dynamics and the choice of boundary layer is provided and; *iv)* a simple simulation procedure is proposed to estimate the minimum boundary layer capable of recovering the ideal SMC performance and avoiding the occurrence of chattering.

Our interest is to solve the Single-Input Single-Output (SISO) problem of attitude tracking of a fighter aircraft, applying the UIR proposed in [24] and extended to Multi-Input Multi-Output (MIMO) in [34]. To the best of the authors knowledge, this problem has not been solved with UIR previously in other works, therefore, it represents the main contribution of this work in conjunction with the aforementioned novelties *i)*, *ii)* and *iii)*. Two approaches are contemplated: an initial approach, without considering unknown parameters, leading to the pure UIR; and another approach, considering uncertainties, in a control derivative. It is worth mentioning that the longitudinal dynamic of the aircraft is presented and a PI controller is used in parallel to keep the total velocity of the aircraft constant as a secondary control objective. This paper is organized as follows: in Section 2, a summarized procedure and a compendium of the assumptions adopted regarding the controller design are presented; then, in Section 3, the aircraft longitudinal model is presented and the control problem is formulated. Section 4 deals with the normal form transformation and the error dynamics. In Section 5, the internal dynamic stability is demonstrated. In section 6 the controller design is developed and the controller parameters are justified and calculated. In Section 7 the demonstration of the system stability (controller+plant) is developed and Section 8 is used to compare the performance of the approaches proposed through simulations, and finally in section 9 the conclusions summarize the main results the work.

2. GENERAL PROCEDURE OF CONTROLLER DESIGN

In this section, the main steps to apply the universal integral regulator to a general system are presented. The methodology is based on the assumptions proposed in the works [24] and [34], specifically for MIMO systems. Consider the nonlinear MIMO system in (1) composed by the state $x \in R^n$, control $u \in R^m$, output $y \in R^m$, unknown constant parameter $\theta \in R^p$ and exogenous signal $w \in R^q$ vectors.

$$\dot{x} = f(x,\theta) + \sum_{j=1}^{m} g_i(x,\theta)[u_i + \delta_i(x,\theta,w)],$$
$$y_i = h_i(x,\theta), \;\; 1 \leq i \leq m. \tag{1}$$

The first assumption is related to the conditions necessary to lead the system to normal form. It can be formulated as

Assumption 1: The system in (1) has a uniform vector relative degree $\{\rho_1, \rho_2, \ldots, \rho_m\}$, determined through (2), and conditions for the system be input-output linearizable must be accomplished, such as, matrix $A(x,\theta) = \{L_{g_j} L_f^{\rho_i - 1} h_i\}$ is non-singular and the distribution span $\{g_1, g_2, \ldots, g_m\}$ is involutive.

$$L_{g_j} L_f^k h_i(x) = 0, \;\; 0 \leq k \leq \rho_i - 2, \;\; 0 \leq i, j \leq m. \tag{2}$$

Remark 1: Equation (2) is also known as Lie derivative. Its solution allows the determination of the relative degree of the system (number of derivatives of the output to find direct relations with the input). Then, it is possible to do a change of variables that allows the transformation of the system to normal form and the local diffeomorphism $T(x,\theta)$ is constructed (see (3)) with $\eta \in R^{n-\rho}$ (internal variables), $\xi \in R^{\rho}$ (external variables) and total relative degree $\rho = \rho_1 + \rho_2 + \ldots \rho_m$. The new external and internal variables are determined using (4) and (5), respectively.

$$\begin{bmatrix} \eta \\ \xi \end{bmatrix} = T(x,\theta) = \begin{bmatrix} T_1(x,\theta) \\ T_2(x,\theta) \end{bmatrix}, \tag{3}$$

$$\xi = \{\xi^i\} = L_f^{j-1} h_i, \;\; 1 \le i \le m, \;\; 1 \le j \le \rho_i, \tag{4}$$

$$L_{g_i}\eta_i = 0, \;\; 1 \le j \le m, \;\; 1 \le i \le (n-\rho). \tag{5}$$

Once the new variables are determined, the next step is to create the new dynamic, which can be done by means of the following transformation (6) presented in [24].

$$\begin{cases} \dot{\xi}_i = \xi_{i+1}, & 1 \le i \le (\rho - 1), \\ \dot{\xi}_\rho = b(\xi,\eta) + a(\xi,\eta)u, & \\ \dot{\eta} = L_f \eta_j, & 1 \le j \le (n-\rho). \end{cases} \tag{6}$$

With $b(\xi,\eta) = L_f^{\rho} h_i(x)$ and $a(\xi,\eta) = L_g L_f^{\rho-1} h_i(x) = A(x)$. The next assumption states the existence of a unique equilibrium point and a unique control input to solve the regulation or tracking problem. This assumption is based on a vector $d \in D_d$ defined as $d = [r_{ss}, \theta, w_{ss}]$ and representing the steady state values of the reference r_i, constant unknown parameters θ and exogenous signal $w(t)$ vectors.

Assumption 2: For each $d \in D_d$there exists a unique equilibrium point $\bar{x} = \bar{x}(d) \in D_x$ and a unique control $\bar{u} = \bar{u}(d)$ such that $f(\bar{x},\theta) + g(\bar{x},\theta)[\bar{u} + \delta(\bar{x},\theta,w_{ss}) = 0$ and $r_{ss} = h(\bar{x},\theta)$.

Remark 2: Assumption 2 supposes that there exists only one control and one equilibrium point in which the system output is able to track the desired reference and this point is used to create the error dynamic necessary to construct the sliding surface.

Then, the error dynamics can be constructed using the change of variables $z = \eta - \bar{\eta}$ for the internal dynamic and $e^i = \xi^i - \bar{\xi}^i - v^i$ for the external dynamic, with $v^i(t) = [r_i - r_{iss}, r_i^{(1)}, \ldots, r_i^{\rho-1}]$. More details about the conditions that must be accomplished to effectively solve the tracking problem can be found in [34]. Some boundaries are defined to for the errors being $e \in E = \{|e| < l_1\}$ and $z \in Z = \{|z| < l_2\}$ where l_1 and l_2 are positive constants independent of d.

In order to demonstrate the stability of the internal dynamic (input-to-state stability), assumption 3 has to be attended to by means of (7).

Assumption 3: There exists a proper function $V_z : Z \to R_+$ possibly dependent on d, and class K functions λ independent of d $\lambda_i : [0, l_2) \to R_+ (i = 1,2,3)$ and $\gamma_i : [0, l_0 + l_1) \to R_+$ such that

$$\begin{aligned} &\lambda_1(|z|) \le V_z(t,z,d) \le \lambda_2(|z|), \\ &\frac{\partial V_z}{\partial t} + \frac{\partial V_z}{\partial z}\phi(z, e+v, d) \le \lambda_3(|z|), \end{aligned} \tag{7}$$

$\forall |z| \ge \gamma(|e+v|)$. So, the equilibrium point of the internal dynamic $z = 0$ of $\dot{z} = \phi(z,0,d)$ is exponentially stable uniformly in d.

Remark 3: Assumption 3 is necessary to guarantee that once the tracking problem is solved, that is, the error is lead to zero, the internal dynamic represented by $\dot{z}$ will converge exponentially to zero. It is worth mentioning that an unstable internal dynamic can affect UIR controller performance.

The next step consists of defining the controller based on the CSMC of (8). The integral variable σ_i represents the output of the conditional integrator in (9). If the first derivative of the sliding surface is taken, the result will be as in (10) with $F_i(z,e,v,d,r^{\rho_i}) = b_i(\cdot) - r_i^{\rho_i} + \{k_0^i\left[-k_0^i\sigma_i + \mu_i sat(s_i/\mu_i)\right]\}$.

$$s_i = k_0^i \sigma_i + \sum_{j=1}^{\rho_i - 1} k_j^i e_j^i + e_{\rho_i}^i, \tag{8}$$

$$\dot{\sigma}_i = -k_0^i \sigma_i + \mu_i sat\left(\frac{s_i}{\mu_i}\right), \;\; k_0^i > 0, \tag{9}$$

$$\dot{s}_i = F_i(z,e,v,d,r^{\rho_i}) + \sum_{j=1}^{m} a_{ij}[u_j + \delta_j(\cdot)]. \tag{10}$$

At this point it is important to highlight the importance of the matrix $A(x) = a_{ij}$. In the case of considering unknown parameters and modelling uncertainties, the matrix $A(x)$ can be substituted by its nominal value $\hat{A}(x)$; for this, assumption 4 should be defined.

Assumption 4: Let $A(z, e+v, d) = \Gamma(z, e+v, d, r_i^{\rho_i})$ $\hat{A}(e+v)$ where the matrix $\hat{A}$ is a known non-singular matrix and $\Gamma = diag[\gamma_1, \gamma_2, \ldots, \gamma_m]$, with $\gamma(\cdot) \ge \gamma_0 > 0, \quad 1 \le i \le m$ for all $e \in E$, $z \in Z$, $d \in D_d$ and some positive constant γ_0.

Remark 4: As explained in [34], Assumption 4 is given to extend the concept of nominal values to MIMO systems. This is done in order to take into account possible uncertainties in the model through the proposition of a non-singular matrix Γ. The non-singular condition guarantees that the application of equivalent control can be done avoiding singularities in the denominator of the control of (11).

By following this line of reasoning, we arrive at the use of the equivalent control method leading to the UIR controller u as defined in (11).

$$\begin{aligned} &u = \hat{A}^{-1}(e,v)[-\hat{F}(e,v,\bar{w}) + v_i], \\ &v_i = -K_i(e,v,\bar{w}) sat(s_i/\mu_i). \end{aligned} \tag{11}$$

Finally, an additional assumption is necessary to determine the controller gain K_i. The expression on (12) will be clear in Section 6.

Assumption 5: Let

$$max\left|\frac{\Delta_i(\cdot)}{\gamma_i(\cdot)}\right| \leq \nu(e,v,\bar{w}),\quad 1\leq i\leq m, \tag{12}$$

where $\{\Delta_i(\cdot)\} = F(\cdot) - \Gamma(\cdot)\hat{F}(\cdot) + A(\cdot)\delta(\cdot) + \{k_0^i[-k_0^i\sigma_i + \mu_i sat(s_i/\mu_i)]\}$ is the resultant term of the first derivative of the sliding surface in (13)

$$\begin{aligned}\dot{s}_i =& \Delta_i(z,e,\bar{w},\sigma,d,\tilde{w})\\ &-\gamma_i(z,e+v,\bar{w})K_i(e,v,\bar{w})sat(s_i/\mu_i).\end{aligned} \tag{13}$$

Remark 5: The purpose of Assumption 5 is to guarantee that $s_i\dot{s}_i < 0$. If we choose a Candidate Lyapunov Function (CLF) $V_s = (1/2)s^2$, the maximization of the $\Delta(\cdot)$ function will allow to determine the controller gain $K_i = \nu(\cdot) + q_i$ (with $q_i > 0$) that is able to ensure that the first derivative of the CLF $\dot{V}_s = s_i\dot{s}_i$ is negative definite attending the asymptotic stability condition done by the Lyapunov direct method.

3. MODEL AND PROBLEM FORMULATION

3.1. Aircraft model

The aircraft dynamics considered in this work is the longitudinal model of a Mirage III fighter aircraft extracted from [35]. The three-degrees-of-freedom mathematical model uses aerodynamic data (stability and control derivatives) which can be considered approximately constant. The model in a combined wind and body axes is described in (14).

$$\begin{aligned}\dot{V} &= \frac{1}{V}(u\dot{u}+v\dot{v}+w\dot{w}),\\ \dot{\alpha} &= \frac{\left(\frac{\dot{w}}{u}-\frac{w\dot{u}}{u^2}\right)}{\sqrt{1+(w/u)^2}},\\ \dot{q} &= c_5pr - c_6(p^2-r^2)+c_7M,\\ \dot{\Theta} &= q\cos\Phi - rsen\phi,\end{aligned} \tag{14}$$

where V is the total velocity of the aircraft, α is the angle of attack, q the pitch rate, Θ the attitude angle and the constants $c_5 = (I_{zz}-I_{xx})/I_{yy}$, $c_6 = I_{xz}/I_{yy}$ and $c_7 = 1/I_{yy}$. In this work, it is assumed that the longitudinal and latero-directional dynamics are decoupled and the latero-directional variables Φ, p and r are approximately zero. The equations of motion of the velocity components u, v and w are represented as follows:

$$\begin{aligned}\dot{u} &= m^{-1}(F_x + T\cos\alpha_f) - gsen\phi + rv - qw,\\ \dot{v} &= m^{-1}F_y + gsen\phi\cos\theta + pw - ru,\\ \dot{w} &= m^{-1}(F_z + Tsen\alpha_f) + g\cos\phi\cos\theta + qu - pv,\end{aligned} \tag{15}$$

Table 1. Aircraft properties.

Property	Value	Property	Value
$m[kg]$	7400	C_{L_q}	0
$S[m^2]$	36	C_{m_0}	0
$\bar{c}[m]$	5.25	C_{m_α}	-0.17
$I_{yy}[kg\cdot m^2]$	5.4×10^4	C_{m_q}	-0.4
C_{L_0}	0	$C_{m_{\delta_p}}$	-0.45
C_{L_α}	2.204	-	-

where m is the aircraft mass, g the acceleration of gravity, T the maximum thrust and α_f the engine incidence angle considered null in this work. The forces F_x, F_y, F_z and the pitch moment M are written as in (16).

$$\begin{aligned}&F_x = \bar{q}SC_x,\quad F_y = \bar{q}SC_y,\\ &F_z = \bar{q}SC_z,\quad M = \bar{q}S\bar{c}C_m,\end{aligned} \tag{16}$$

where $\bar{q}$ denotes the dynamic pressure and S and $\bar{c}$ the wing surface and mean aerodynamic chord, respectively. The aerodynamic coefficients C_x, C_y, C_z and C_m are functions of the Euler angles and the aerodynamic coefficients C_L, C_D and C_ya which in turn depend on the stability derivatives C_{m_0}, C_{m_α}, C_{m_q}, control derivative $C_{m_{\delta_p}}$ and control input δ_p. Some physical properties and aerodynamic data of the model are shown in Table 1.

Expanding (14) and using Equations 15 and 16 the system can be written as in (17) below:

$$\begin{aligned}\dot{\alpha} &= q + \frac{g}{V}\cos(\alpha-\Theta) - \frac{T}{mV}\sin\alpha\\ &\quad + \frac{\bar{q}S}{mV}C_L(\alpha,q) - \left(\frac{T}{mV}\sin\alpha\right)\delta_\pi,\\ \dot{q} &= \frac{\bar{q}S\bar{c}}{I_{yy}}\left[C_{m_0} + C_{m_\alpha}\alpha + C_{m_q}\left(\frac{\bar{c}}{V}\right)q\right]\\ &\quad + \left(\frac{\bar{q}S\bar{c}}{I_{yy}}C_{m_{\delta_p}}\right)\delta_p,\\ \dot{\Theta} &= q.\end{aligned} \tag{17}$$

It should be noted that the velocity dynamic is not considered in (17). A parallel proportional integrative (PI) controller will be used to keep the aircraft total velocity constant using the thrust deflection δ_π as a secondary objective.

3.2. Problem formulation

Consider the system in (17). This system can be rewritten in the input affine-form $\dot{x} = f(x) + g(x)u$ with the state vector $x \in R^n$ $(n=3)$ as $x = \{\alpha, q, \Theta\}^T$, the control input vector $u \in R^m$ $(m=1)$ as $u = \{\delta_p\}$, and to complete the SISO problem, the output vector $y \in R^p$ $(p=m)$ as $y = h(x) = \{\Theta\}$. With the smooth functions

$f(x) = [f_1, f_2, f_3]^T$ and $g(x) = [g_1, g_2, g_3]^T$ showed in (18).

$$f(x) = \begin{bmatrix} q + \frac{g}{V}\cos(\alpha - \Theta) - \frac{T}{mV}\sin\alpha \\ + \frac{\bar{q}S}{mV} C_L(\alpha, q)\left(\frac{T}{mV}\sin\alpha\right)\delta_\pi \\ \frac{\bar{q}S\bar{c}}{I_{yy}}\left[C_{m_0} + C_{m_\alpha}\alpha + C_{m_q}\left(\frac{\bar{c}}{V}\right)q\right] \\ q \end{bmatrix},$$

$$g(x) = \begin{bmatrix} 0 \\ \frac{\bar{q}S\bar{c}}{I_{yy}} C_{m_{\delta_p}} \\ 0 \end{bmatrix}. \tag{18}$$

The control problem consists in designing the elevator control that makes the attitude angle Θ to track a reference doublet "smoothed" through a first order filter. Here the filter $H(s) = \frac{1}{\tau s + 1}$ with time constant $\tau = 1$ was used, this filter smoothing is important to ensure that the first derivative of the error is bounded. The control problem must be solved ensuring that the internal dynamic of the system is input-to-state stable and guaranteeing asymptotic stability of the external error. In order to better formulate the control problem it is assumed that the system has uniform relative degree and can be converted to normal form (Assumption 1). Another assumption considered in this work to simplify the control problem is:

Assumption 6: All the latero-directional state variables are null or constant and only the longitudinal states are time varying, therefore, the longitudinal and latero-directional dynamics are decoupled.

4. NORMAL FORM TRANSFORMATION AND TRACKING PROBLEM

4.1. Normal form transformation

Using Assumption 1 and the Lie derivative of (2) as proposed in [21] and [24], we can compute the relative degree to the output $y = h(x) = \{\Theta\}$, then, for $k = 0$ we have $L_g h(x) = g_3 = 0$ which does not attend (2). For $k = 1$, the Lie derivative becomes $L_g L_f h(x) = g_2 = A(x)$, resulting in a relative degree $\rho = k + 1 = 2$. Due to $\rho < n$ the transformation is partial and we have internal and external dynamics.

The new internal and external variables are determined by means of (19) and (20). The new external variables are computed in (21).

$$\xi_j^i = L_f^{j-1} h_i, \quad \begin{cases} 1 \le j \le \rho, \\ 1 \le i \le m, \end{cases} \tag{19}$$

$$L_g \eta = 0, \tag{20}$$

$$\xi_1 = L_f^0 h(x) = h(x) = \Theta,$$

$$\xi_2 = L_f h(x) = \begin{bmatrix} \frac{\partial \Theta}{\partial \alpha} & \frac{\partial \Theta}{\partial q} & \frac{\partial \Theta}{\partial \Theta} \end{bmatrix} \begin{bmatrix} f_1 \\ f_2 \\ f_3 \end{bmatrix} = q. \tag{21}$$

With f_1, f_2 and f_3 as defined in (18). It is easy to check that the simplest choice $\eta = \alpha$ satisfies the condition 20, by the fact that $g_1 = g_3 = 0$ and the choice of η does not depend on q, see (22).

$$L_g \eta = \frac{\partial \eta}{\partial \alpha} g_1 + \frac{\partial \eta}{\partial q} g_2 + \frac{\partial \eta}{\partial \Theta} g_3 = 0. \tag{22}$$

In accordance with [24] the new external and internal dynamics are constructed as in (23) and (25) respectively, and the normal form transformation is completed.

$$\begin{aligned} \dot{\xi}_1 &= \xi_2, \\ \dot{\xi}_2 &= b(\xi, \eta) + a(\xi, \eta) u, \end{aligned} \tag{23}$$

where $b(\xi, \eta)$ and $a(\xi, \eta)$ as in (24).

$$\begin{aligned} b(\xi, \eta) &= L_f^2 h(x) = \frac{\bar{q}S\bar{c}}{I_{yy}}\left[C_{m_0} + C_{m_\alpha}\eta + C_{m_q}\left(\frac{\bar{c}}{V}\right)\xi_2\right], \\ a(\xi, \eta) &= L_g L_f h(x) = A(x) = g_2 = \frac{\bar{q}S\bar{c}}{I_{yy}} C_{m_{\delta_p}}, \end{aligned} \tag{24}$$

$$\begin{aligned} \dot{\eta} &= \begin{bmatrix} \frac{\partial \alpha}{\partial \alpha} & \frac{\partial \alpha}{\partial q} & \frac{\partial \alpha}{\partial \Theta} \end{bmatrix} \begin{bmatrix} f_1 \\ f_2 \\ f_3 \end{bmatrix} = f_1 \\ &= \xi_2 + \frac{g}{V}\cos(\eta - \xi_1) - \frac{T}{mV}\sin\eta \\ &\quad - \frac{\bar{q}S}{mV} C_L(\alpha, q) - \left(\frac{T}{mV}\sin\alpha\right)\delta_\pi. \end{aligned} \tag{25}$$

4.2. Tracking problem

Through Assumption 2, it is possible to define the error dynamics. Let $z = \eta - \bar{\eta}$ be the internal dynamic error with $\bar{\eta} = \alpha_{eq}$ and $e_i = \xi_i - \bar{\xi}_i - v_1$ the external dynamic error with $\bar{\xi}_1 = [r_{1ss}, 0] = [\Theta_{eq}, 0]$ and $v_1 = [r_1 - r_{1ss}, r_1'] = [\Theta_{ref} - \Theta_{eq}, \Theta_{ref}']$ where Θ_{ref}' is the time derivative of the attitude reference. Finally, the system error is as presented in (26) and the error dynamics can be written in the compact matrix form (27).

$$e = [e_1, e_2] = [\xi_1 - \Theta_{ref}, \xi_2 - \Theta_{ref}'], \tag{26}$$

$$\begin{Bmatrix} \dot{e}_1^\Theta \\ \dot{e}_2^\Theta \end{Bmatrix} = \begin{bmatrix} 0 & 1 \\ 0 & 0 \end{bmatrix} \begin{Bmatrix} e_1^\Theta \\ e_2^\Theta \end{Bmatrix} + \begin{bmatrix} 0 \\ 1 \end{bmatrix} \{b(e, \eta) + a(e, \eta) u\}. \tag{27}$$

5. INTERNAL DYNAMIC STABILITY DEMONSTRATION

In this section we will demonstrate that the internal dynamic of the system is exponentially stable using Assumption 3. This is necessary because the procedure adopted to design the UIR in this paper is applicable only to minimum-phase nonlinear systems [34]. The internal dynamics of the system is represented by (28).

$$\dot{z} = \phi(z, e + v, d)$$

$$
\begin{aligned}
&= e_2 + \Theta'_{ref} + \frac{g}{V}\cos(z+\alpha_{eq}-e_1-\Theta_{ref}) \\
&\quad - \frac{T}{mV}\sin(z+\alpha_{eq}) \\
&\quad - \frac{\bar{q}S}{mV}C_L(\alpha,q) - \frac{T}{mV}\sin(z+\alpha_{eq})\delta_\pi. \qquad (28)
\end{aligned}
$$

For convenience, the following constants $\bar{c_1}, \bar{c_2}, \bar{c_3}, \bar{a}$ and $\bar{b}$ are defined in (29). Then the internal dynamic is rewritten as in (30).

$$
\begin{aligned}
&\bar{c_1} = \frac{g}{V},\ \ \bar{c_2} = \frac{T}{mV}(1+\delta_\pi) \quad \bar{c_3} = \frac{\bar{q}S}{mV}C_L(\alpha,q), \\
&\bar{a} = (z+\alpha_{eq}-e_1-\Theta_{ref}),\ \ \bar{b} = (z+\alpha_{eq}), \qquad (29) \\
&\dot{z} = \phi(z,e+v,d) = e_2 + \bar{c_1}cos\bar{a} - \bar{c_2}sen\bar{b} - \bar{c_3} + \Theta'_{ref}. \qquad (30)
\end{aligned}
$$

We proceed to prove that the equilibrium point $z=0$ of the non-observable dynamic ("zero dynamic" with $e=0$ and $v=0$) $\dot{z}=\phi(z,0,d)$ (see (31)), is exponentially stable, for this purpose the conditions stated in Assumption 3 must be attended.

$$
\begin{aligned}
\dot{z} &= \phi(z,0,d) \\
&= \bar{c_1}\cos(z+\alpha_{eq}) - \bar{c_2}\sin(z+\alpha_{eq}) - \bar{c_3}(z+\alpha_{eq}). \qquad (31)
\end{aligned}
$$

Let $V_z = \frac{1}{2}z^T z$ be a candidate Lyapunov function (CLF) for z. There exist two class K functions $\lambda_1 = \frac{\pi}{10}|z|^2$ and $\lambda_2 = \frac{\pi}{4}|z|^2$ such that $\lambda_1 \leq V_z \leq \lambda_2$. Deriving the CLF we obtain the (32) below:

$$
\begin{aligned}
\dot{V}_z &= z\dot{z} \\
&= z[\bar{c_1}\cos(z+\alpha_{eq}) - \bar{c_2}\sin(z+\alpha_{eq}) \\
&\quad - \bar{c_3}(z+\alpha_{eq})] \\
&= z\bar{c_1}\cos(z+\alpha_{eq}) - z\bar{c_2}\sin(z+\alpha_{eq}) \\
&\quad - \bar{c_3}z^2 - z\alpha_{eq}\bar{c_3} \\
&= |z||\bar{c_1}\cos(z+\alpha_{eq})| \\
&\quad - |z|(|\bar{c_2}\sin(z+\alpha_{eq})| + \alpha_{eq}|\bar{c_3}|) - |\bar{c_3}||z|^2. \qquad (32)
\end{aligned}
$$

It is easy to see that the critical case occurs when $cos(z+\alpha_{eq}) >> sin(z+\alpha_{eq})$, this is, with $z=-\alpha_{eq}$, in this case of $cos(z+\alpha_{eq})=1$ and $sin(z+\alpha_{eq})=0$. Due to $\alpha_{eq}>0$ ($C_{L_0}=0$ see Table 1) as result:

$$
\begin{aligned}
\dot{V}_z &= z\dot{z} \\
&= z\bar{c_1} - z\alpha_{eq}\bar{c_3} - \bar{c_3}z^2 \\
&\leq -\alpha_{eq}|\bar{c_1}| + \alpha_{eq}^2|\bar{c_3}| - \alpha_{eq}^2|\bar{c_3}| \\
&\leq -\alpha_{eq}|\bar{c_1}| = -\lambda_3. \qquad (33)
\end{aligned}
$$

Due to $\alpha_{eq}>0$ and $|\bar{c_1}| = g/V > 0 \quad \forall V>0$, $\dot{V}_z$ is negative definite, the internal dynamic is exponentially stable, therefore, when $e_1, e_2 \to 0$, the internal error $z \to 0$.

Performing a deeper analysis, it is easy to check that when $z=0$ the derivative of the CLF is: $\dot{V} \leq -\lambda_3|z|^2$ with $\lambda_3 = \bar{c_3} > 0 \quad \forall\alpha>0$, where $\alpha=\alpha_{eq}>0$. In the case of $z>0$ we have: $\alpha>\alpha_{eq}$, due to the angle of attack is bounded between the interval $-\pi/18 < \alpha < \pi/4$ and in the boundary $\alpha = [\alpha_{eq} \quad \pi/4]$, the $cos(z+\alpha_{eq}) > sin(z+\alpha_{eq})$ the maximum difference occurs at $\alpha \approx \alpha_{eq}$, then $cos(\alpha_{eq}) \approx 1$ e $sin(\alpha_{eq}) \approx \alpha_{eq}$, and finally:

$$
\begin{aligned}
\dot{V}_z &= |z||\bar{c_1}cos(\alpha_{eq})| - |z|(|\bar{c_2}sin(\alpha_{eq})| + \alpha_{eq}|\bar{c_3}|) \\
&\quad - |\bar{c_3}||z|^2 \\
&\leq |z||\bar{c_1}| - |z|\alpha_{eq}(|\bar{c_2}|+|\bar{c_3}|) - |\bar{c_3}||z|^2 \\
&\quad \text{with } \alpha_{eq}(|\bar{c_2}|+|\bar{c_3}|) > |\bar{c_1}| \\
&\leq -\lambda_3|z|^2, \text{ where } \lambda_3 = |\bar{c_3}|. \qquad (34)
\end{aligned}
$$

From (32), (33), and (34) we conclude that, internal dynamic is exponentially stable due to $V_z \geq 0$ and $\dot{V}_z \leq \lambda_3^{min} = min\{\alpha_{eq}|\bar{c_1}|, |\bar{c_3}|\} > 0$. Then, $z \to 0$ while $e_1, e_2 \to 0$, that is, the internal dynamic will not affect the controller performance. In the following steps two approaches are proposed to design the controller and determine the controller parameters.

6. CONTROLLER DESIGN

6.1. Case 1: approach without considering unknown parameters

The first step is to design the sliding surface of CSMC (35) modified by the introduction of a conditional integrator whose variable is defined as σ_Θ. Using the relative degree previously computed $\rho=2$, (36) is obtained.

$$
s_\Theta = k_0^\Theta\sigma_\Theta + \sum_{j=1}^{\rho-1} k_j^\Theta e_j^\Theta + e_\rho^\Theta \quad 1 \leq j \leq \rho-1, \qquad (35)
$$

$$
s_\Theta = k_0^\Theta\sigma_\Theta + k_1^\Theta e_1^\Theta + e_2^\Theta, \qquad (36)
$$

where $e_2^\Theta = \dot{e}_1^\Theta$. The constant $k_1^\Theta > 0$ is chosen such that the polynomial $k_1^\Theta + \lambda_1^\Theta = 0$ has only roots with negative real parts. Deriving the sliding surface we obtain (see (37)):

$$
\dot{s}_\Theta = k_0^\Theta\dot{\sigma}_\Theta + k_1^\Theta e_2^\Theta + \dot{e}_2^\Theta. \qquad (37)
$$

Keeping in mind that the conditional integrator dynamics is defined by $\dot{\sigma}_\Theta = -k_0^\Theta\sigma_\Theta + \mu_\Theta sat\,(s_\Theta/\mu_\Theta)$ and using $\dot{e}_2^\Theta$ from (27):

$$
\begin{aligned}
\dot{s}_\Theta &= k_0^\Theta\left\{-k_0^\Theta\sigma_\Theta + \mu_\Theta sat\,(s_\Theta/\mu_\Theta)\right\} + k_1^\Theta e_2^\Theta \\
&\quad + b(e,\eta) + a(e,\eta)u_\Theta. \qquad (38)
\end{aligned}
$$

Assuming that $a(e,\eta) = A(x) = g_2$ is completely known in (38), we define the UIR controller as in (39).

$$
\begin{cases}
u_\Theta = g_2^{-1}\left[-\hat{F}(\cdot) + v_\Theta\right], \\
v_\Theta = -K_\Theta sat\left(\frac{s_\Theta}{\mu_\Theta}\right).
\end{cases} \qquad (39)
$$

Due to the flexibility of choosing $\hat{F}(\cdot) = 0$ for SISO systems [34], the controller will be as in (40).

$$u_\Theta = -g_2^{-1} K_\Theta sat\left(\frac{s_\Theta}{\mu_\Theta}\right). \quad (40)$$

With $K_\Theta = \nu_\Theta(\cdot) + q_\Theta$ and $q_\Theta > 0$ as stated in Assumption 5. Substituting u_Θ in $\dot{s}_\Theta$ of (38) and analyzing outside the boundary layer ($|s_\Theta| \le \mu_\Theta$), we have $F_\Theta(\cdot) = k_1^\Theta e_2^\Theta + b(e,\eta)$, in this region $sat\,(s_\Theta/\mu_\Theta) = s_\Theta/|s_\Theta|$, then the derivative of the CLF will be as showed in (41).

$$\dot{s}_\Theta = \Delta_\Theta(\cdot) - K_\Theta(s_\Theta/|s_\Theta|), \quad (41)$$

where $\Delta_\Theta(\cdot) = k_0^\Theta\left\{-k_0^\Theta \sigma_\Theta + \mu_\Theta sat\,(s_\Theta/\mu_\Theta)\right\} + F_\Theta(\cdot)$. It will be demonstrated later in the stability demonstration for s_Θ that $s_\Theta \dot{s}_\Theta < 0$, then it is necessary to define $\nu_\Theta(\cdot)$ as in (42) (See Assumption 5).

$$\nu_\Theta(\cdot) \ge max\left|\Delta_\Theta(\cdot)\frac{|s_\Theta|}{s_\Theta}\right| = max\left|\Delta_\Theta(\cdot)\right|. \quad (42)$$

Maximizing $\Delta_\Theta(\cdot)$ (See (43)).

$$\begin{aligned}
\Delta_\Theta(\cdot) &= \frac{|s_\Theta|}{s_\Theta} k_0^\Theta \left\{-k_0^\Theta \sigma_\Theta + \mu_\Theta \frac{s_\Theta}{|s_\Theta|}\right\} + \frac{|s_\Theta|}{s_\Theta} F_\Theta(\cdot) \\
&= -\left(k_0^\Theta\right)^2 \sigma_\Theta \frac{|s_\Theta|}{s_\Theta} + k_0^\Theta \mu_\Theta + \frac{|s_\Theta|}{s_\Theta} F_\Theta(\cdot) \\
&\le k_0^\Theta \mu_\Theta - sign(s_\Theta) k_0^\Theta \mu_\Theta + \frac{|s_\Theta|}{s_\Theta} F_\Theta(\cdot) \\
&\le 2k_0^\Theta \mu_\Theta + |F_\Theta(\cdot)|. \quad (43)
\end{aligned}$$

We choose $q_\Theta = 2.1 k_0^\Theta \mu_\Theta > 0$ to overbound the term $2k_0^\Theta \mu_\Theta$ and $\nu_\Theta(\cdot)$ will be $\nu_\Theta(\cdot) \ge |F_\Theta(\cdot)| = k_1^\Theta \left|e_2^\Theta\right| + |b(e,\eta)|$. Finally we determine the controller gain by means of $K_\Theta = \nu_\Theta(\cdot) + q_\Theta$.

6.2. Case 2: approach considering unknown parameters

By means of Assumption 4 we will consider that $a(\cdot)$ is not totally known, therefore, an unknown parameter is defined. Let $\theta \in [\theta_i^m, \theta_i^M]$ $(i = 1)$ be the unknown parameters vector. In this work, the only unknown parameter considered is $\theta_1 = Cm_{\delta p}$, then $a(\cdot) = g_2 = k_a \theta_1$ with $k_a = \frac{\bar{q}S\bar{c}}{I_{yy}}$.

Assuming that $a(\cdot)$ is not exactly known, we define a nominal value $\hat{a}(\cdot)$ which satisfies the equation $a(\cdot) = \Gamma(\cdot)\hat{a}(\cdot)$, logically $\Gamma(\cdot) = \frac{a(\cdot)}{\hat{a}(\cdot)} = \frac{\theta_1}{\hat{\theta}_1}$. Due to $F_\Theta(\cdot)$ and $b(e,\eta)$ are not dependent on θ, then, $\hat{F}_\Theta(\cdot) = F_\Theta(\cdot)$ and $\hat{b}(e,\eta) = b(e,\eta)$ with $F_\Theta(\cdot)$ and $b(e,\eta)$ as in (44).

$$\begin{aligned}
F_\Theta(\cdot) &= k_1^\Theta e_2^\Theta + b(e,\eta), \\
b(e,\eta) &= k_a\left[C_{m_0} + C_{m_\alpha}\eta + C_{m_q}\left(\frac{\bar{c}}{V}\right)(e_2^\Theta + \Theta'_{ref})\right]. \quad (44)
\end{aligned}$$

In the case of functions $F_\Theta(\cdot)$ and $b(e,\eta)$ be dependent on θ, its corresponding $\hat{F}_\Theta(\cdot)$ and $\hat{b}(e,\eta)$ need to be calculated. Once these considerations are taken into account, the controller presented in (40) becomes (45).

$$u_\Theta = \frac{-\hat{F}_\Theta(\cdot) - K_\Theta sat(s_\Theta/\mu_\Theta)}{\hat{a}(\cdot)}. \quad (45)$$

Substituting it in the first derivative of the sliding surface, we obtain the Expression on (46) below:

$$\begin{aligned}
\dot{s}_\Theta =& k_0^\Theta\left\{-k_0^\Theta \sigma_\Theta + \mu_\Theta sat\,(s_\Theta/\mu_\Theta)\right\} + F_\Theta(\cdot) \\
&- \Gamma(\cdot)\hat{F}_\Theta(\cdot) - \Gamma(\cdot)\hat{F}_\Theta(\cdot) K_\Theta sat(s_\Theta/\mu_\Theta). \quad (46)
\end{aligned}$$

Analyzing (46) it can be understood that in the case of $a(\cdot) = \hat{a}(\cdot)$, that is, $a(\cdot)$ is precisely known, the parameter $\Gamma(\cdot) = 1$ leads to the cancellation of the terms $F_\Theta(\cdot) - \Gamma(\cdot)\hat{F}_\Theta(\cdot)$. In case 2 we will assume that $a(\cdot) \ne \hat{a}(\cdot)$, then, outside the boundary layer ($|s_\Theta| \ge \mu_\Theta$) the first derivative of the sliding surface will be as in (47).

$$\begin{aligned}
\dot{s}_\Theta =& k_0^\Theta\left\{-k_0^\Theta \sigma_\Theta + \mu_\Theta sat\,(s_\Theta/\mu_\Theta)\right\} \\
&+ F_\Theta(\cdot)[1 - \Gamma(\cdot)] - K_\Theta sat(s_\Theta/\mu_\Theta) \\
=& \underbrace{\left[-(k_0^\Theta)^2 \sigma_\Theta \frac{|s_\Theta|}{s_\Theta} + k_0^\Theta \mu_\Theta\right]\frac{\hat{\theta}_1}{\theta_1} + F_\Theta(\cdot)\frac{|s_\Theta|}{s_\Theta}[1 - \Gamma(\cdot)]\frac{\hat{\theta}_1}{\theta_1}}_{\hat{\Delta}_\Theta(\cdot)} - K_\Theta. \quad (47)
\end{aligned}$$

Once again, to guarantee $\dot{V}_s = s_\Theta \dot{s}_\Theta < 0$, and taking advantage of previous results in (43), K_Θ is computed as showed in (48).

$$\begin{aligned}
K_\Theta =& \hat{\nu}_\Theta(\cdot) + \hat{q}_\Theta \\
=& max\left|\frac{\hat{\theta}_1}{\theta_1}\hat{\Delta}_\Theta(\cdot)\right| + \frac{\hat{\theta}_1}{\theta_1}\hat{q}_\Theta \\
=& \left(\frac{\hat{\theta}_1}{\theta_1} - 1\right)\left(k_1^\Theta\left|e_2^\Theta\right| + |b(e,\eta)|\right) \\
&+ 2k_0^\Theta \mu_\Theta\left(\frac{\hat{\theta}_1}{\theta_1}\right). \quad (48)
\end{aligned}$$

As a consequence, the higher the uncertainty, the higher the controller gain K_Θ, it also can be seen that the higher the boundary layer μ_Θ, the higher the gain K_Θ has to be in order to keep $\dot{V}_s < 0$.

7. STABILITY DEMONSTRATION

The system is written in closed loop form using the error $\zeta \in R^{\rho-1}$ where $\zeta = \{e_i\}; (1 \le i \le \rho - 1)$ [23]. Then, $\zeta_\Theta = e_1^\Theta$, with $s_\Theta = k_0^\Theta \sigma_\Theta + k_1^\Theta e_1^\Theta + e_2^\Theta$ e $e_2^\Theta = \dot{e}_2^\Theta$ we have the new error dynamic as in (49).

$$\dot{\zeta}_\Theta = -k_1^\Theta \zeta_\Theta + (s_\Theta - k_0^\Theta \sigma_\Theta) = M_\Theta + C_\Theta(s_\Theta - k_0^\Theta \sigma_\Theta). \quad (49)$$

M_Θ is always negative by the fact of $k_1^\Theta > 0$ and $C_\Theta = 1$. In order to demonstrate the system stability it is necessary to define the following CLFs (50).

$$V_s = \frac{1}{2}s_\Theta^2;\ \ V_\sigma = \frac{1}{2}\sigma_\Theta^2;\ \ V_\zeta = \zeta_\Theta^T Q \zeta_\Theta \tag{50}$$

such that $Q = Q^T > 0$ can satisfy the Lyapunov equation $QM_\Theta + M_\Theta^T Q = -I$ where $M_\Theta = -k_1^\Theta$.

In the case of the **sliding surface**, it will be demonstrated that the compact set $V_s \leq \frac{1}{2}c_\Theta^2$ with $c_\Theta > \mu_\Theta$ is a positive invariant set. Outside the boundary layer $|s_\Theta| \geq \mu_\Theta$ and $sat(s_\Theta/\mu_\Theta) = s_\Theta/|s_\Theta|$ the first derivative of the sliding surface with $K_\Theta > |\Delta_\Theta(\cdot)| + q_\Theta$ and $q_\Theta > 0$ becomes:

$$\begin{aligned}\dot{V}_s &= s_\Theta \dot{s}_\Theta \\ &= s_\Theta\left(\Delta_\Theta(\cdot) - K_\Theta \frac{s_\Theta}{|s_\Theta|}\right) \\ &\leq |s_\Theta|\,|\Delta_\Theta(\cdot)| - |s_\Theta|\,(|\Delta_\Theta(\cdot)| + q_\Theta)\,\frac{s_\Theta}{|s_\Theta|} \\ &\leq |s_\Theta|\,|\Delta_\Theta(\cdot)| - |s_\Theta|\,|\Delta_\Theta(\cdot)| - q_\Theta\,|s_\Theta| \\ &\leq -q_\Theta\,|s_\Theta| < 0.\end{aligned} \tag{51}$$

Then, due to the first derivative of the CLF in (51) being negative definite, the set $V_s \leq \frac{1}{2}c_\Theta^2$ is positive invariant, that is, any trajectory starting inside this set, will stay inside it for all future time.

For the **conditional integrator**, the compact set $V_\Theta \leq \frac{1}{2}(\mu_\Theta/k_0^\Theta)^2$ is proposed due to $|\sigma_\Theta| \leq (\mu_\Theta/k_0^\Theta)$. As the conditional integrator only provides integral action inside the boundary layer, $|s_\Theta| \leq \mu_\Theta$. Then, $sat(s_\Theta/\mu_\Theta) = s_\Theta/\mu_\Theta$. Deriving the CLF:

$$\begin{aligned}\dot{V}_\sigma &= \sigma_\Theta \dot{\sigma}_\Theta \\ &= \sigma_\Theta\left(-k_0^\Theta \sigma_\Theta + s_\Theta\right) \\ &= -k_0^\Theta \sigma_\Theta^2 + \sigma_\Theta s_\Theta \\ &\leq -k_0^\Theta\,|\sigma_\Theta|^2 + |s_\Theta|\,|\sigma_\Theta| \text{ due to } |s_\Theta| \leq \mu_\Theta \\ &\leq -k_0^\Theta\,|\sigma_\Theta|^2 + \mu_\Theta\,|\sigma_\Theta|.\end{aligned} \tag{52}$$

In Fig. 1 it is possible to see the positive and negative parts of $\dot{V}_\sigma$ in the last inequation of (52). It is noticed that the positive part $\mu_\Theta|\sigma_\Theta|$ is always higher for $\sigma_\Theta \leq (\mu_\Theta/k_0^\Theta)$, on the other hand, for $\sigma_\Theta > (\mu_\Theta/k_0^\Theta)$ the negative part dominates and we can guarantee that $\dot{V}_\sigma < 0$ is negative definite, that is, for any trajectory starting outside the set $V_\Theta \leq \frac{1}{2}(\mu_\Theta/k_0^\Theta)^2$ it will stay inside for all future time. According to [36] (Section 4.8), the system is *Uniformly Ultimately Bounded* and the set is an invariant positive set.

For the stability demonstration of the **closed-loop error** ζ_Θ, the first step is to calculate the Q value in the CLF V_ζ of equation 50. Solving the Lyapunov equation $QM_\Theta + M_\Theta^T Q = -I$ with $M_\Theta = -k_1^\Theta$ e $C_\Theta = 1$, we obtain: $Q = \frac{1}{2k_1^\Theta}$.

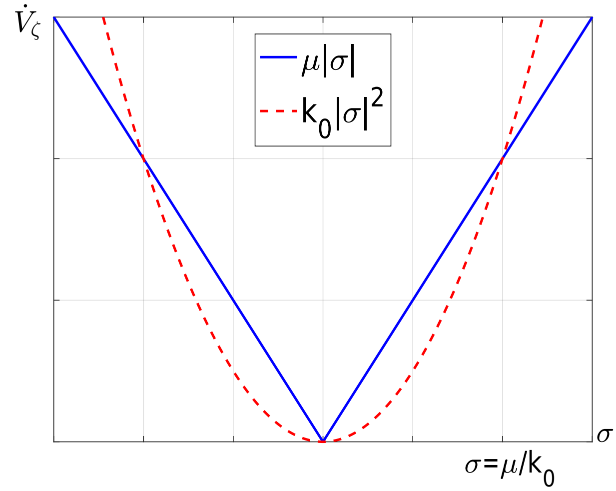

Fig. 1. First derivative parts of CLF of σ_Θ.

Deriving the CLF:

$$\begin{aligned}\dot{V}_\zeta =& \dot{\zeta}_\Theta^T Q \zeta_\Theta + \zeta_\Theta^T Q \dot{\zeta}_\Theta \\ =& \left[M_\Theta^T \zeta_\Theta^T + C_\Theta^T (s_\Theta - k_0^\Theta \sigma_\Theta)^T\right] Q \zeta_\Theta \\ &+ \dot{\zeta}_\Theta^T Q \left[M_\Theta \zeta_\Theta + C_\Theta (s_\Theta - k_0^\Theta \sigma_\Theta)\right] \\ =& \underline{\zeta_\Theta^T M_\Theta^T Q \zeta_\Theta} + Q C_\Theta^T (s_\Theta - k_0^\Theta \sigma_\Theta)^T \zeta_\Theta \\ &+ \underline{\zeta_\Theta^T Q M_\Theta \zeta_\Theta} + \zeta_\Theta^T Q C_\Theta (s_\Theta - k_0^\Theta \sigma_\Theta) \\ =& \underbrace{\zeta_\Theta^T \left[Q M_\Theta + M_\Theta^T Q\right] \zeta_\Theta}_{\text{Lyapunov equation}} + 2 Q C_\Theta (s_\Theta - k_0^\Theta \sigma_\Theta) \zeta_\Theta \\ =& -\zeta_\Theta^T I \zeta_\Theta + 2 Q C_\Theta (s_\Theta - k_0^\Theta \sigma_\Theta) \zeta_\Theta \\ \leq& -|\zeta_\Theta|^2 + 2\,|QC_\Theta|\,(|s_\Theta| + k_0^\Theta\,|\sigma_\Theta|)\,|\zeta_\Theta|.\end{aligned} \tag{53}$$

For the right side of the last inequality in (53) to be zero, it is necessary that $\zeta_\Theta = 2\,|QC_\Theta|\,(|s_\Theta| + k_0^\Theta\,|\sigma_\Theta|) = \delta$, keeping in mind that $|s_\Theta| \leq c_\Theta$ and $|\sigma_\Theta| \leq (\mu_\Theta/k_0^\Theta)$ then, $\delta = 2\,|QC_\Theta|\,(c_\Theta + \mu_\Theta)$. Finally the set $V_\zeta(\delta) \leq \lambda_{max}(Q)\delta^2 = 4\,|QC_\Theta|^2\,(c_\Theta + \mu_\Theta)^2 \lambda_{max}(Q)$ is positive invariant $\forall\,|\zeta_\Theta| \geq \delta$ in a similar manner to the *Uniformly Ultimately Bounded* stability of the conditional integrator.

We can conclude that either the sliding surface, the conditional integrator or the tracking error will converge to its respective equilibrium points with the choice of the parameters $q_\Theta > 0$, $k_0^\Theta > 0$ and $k_1^\Theta > 0$. Then, the compact sets $V_s \leq \frac{1}{2}c_\Theta^2$, $V_\Theta \leq \frac{1}{2}(\mu_\Theta/k_0^\Theta)^2$ and $V_\zeta(\delta) \leq \lambda_{max}(Q)\delta^2$ are positive invariant sets and can be taken as estimations of the system's region of attraction.

8. NUMERICAL SIMULATIONS

As previously stated, the main control objective of the UIR controller designed in this paper is to track a doublet reference signal of attitude angle "smoothed" through a pre-filter $H(s)$ of maximum amplitude of 20°. The numerical parameters adopted (case 1 and 2) are: $|\alpha| \leq 45^\circ$,

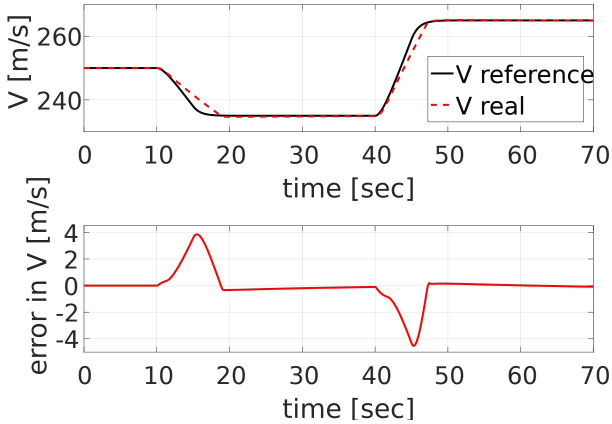

Fig. 2. Velocity response using PI controller.

$|q| \le 90^\circ/s$, $|\theta_1| = Cm_{\delta p} = -0.45$, $\hat{\theta}_1 = -0.5$, $\theta_1^M = -0.3$, $\theta_1^m = -0.7$, the controller parameters: $\mu_\Theta = \pi/4$, $k_0^\Theta = k_1^\Theta = 1$, for case 1, the computed controller gain (using (43)) was $K_\Theta = 13.425$ and for case 2 (using (48)) was $K_\Theta = 3.166$. It is important to remark that the model used in simulations incorporates an actuator with position and rate saturation, therefore, robustness to unmodeled dynamics will be demonstrated.

The proportional and integrative gains of the PI controller were respectively: $K_p = 3$ and $K_I = 0.08$. These were obtained by a trial-and-error process, (54) represents the PI controller which was used to keep the aircraft velocity constant (Mach-hold autopilot). Fig. 2 shows the response of the PI controller tracking the total reference velocity, the controller shows a good performance with a maximum tracking error of 4 m/s. It is worth mentioning that the commanded maneuver in the simulation is more complex than a simple constant velocity, therefore, it is expected to obtain better results in the main tracking problem.

$$u_{PI} = K_p e_1^\Theta + K_I \int_0^t e_1^\Theta dt. \tag{54}$$

In accordance with [34] the boundary layer value μ should be chosen "sufficiently small" in order for the CSMC to recover the performance of the ideal SMC. To do this, and as a novelty in this paper, we will justify the chosen μ value $\mu_\Theta = \pi/4$ through simulations, this simple test will allow us to predict which value of μ makes the chattering phenomenon appear, indicating that the $sat(\cdot) \approx sign(\cdot)$ complying with the subjective criterion previously mentioned.

Several values of μ_Θ are proposed and the corresponding analytical gains K_θ for each μ_Θ are determined (see Table 2). With these parameters and under the trim condition $(\hat{V}, \hat{H}) = (250\ \text{m/s}, 5000\ \text{m})$ the time history of the attitude tracking error and output control signal δ_p are plotted, as showed in Fig. 3.

Table 2. K_Θ for different μ values.

	μ_Θ	K_Θ
$(1/4)\mu$	$\pi/16$	12.325
$(1/2)\mu$	$\pi/8$	12.688
μ	$\pi/4$	13.425
2μ	$\pi/2$	15.225
4μ	π	18.488

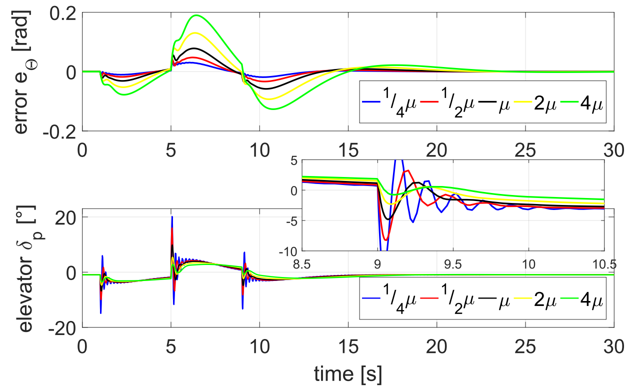

Fig. 3. Tracking error and control signal for various boundary layers.

It is easy to check that the lower the boundary layer value is, the lower the tracking error becomes, this can be explained by the fact that the ideal SMC dominates the controller dynamics. On the other hand, for the lower values $(1/4)\mu$ and $(1/2)\mu$ the control signal suffers chattering (more control oscillation) and higher control demands, this indicates that μ is small enough and that $sat(\cdot) \approx sign(\cdot)$. In order to avoid the chattering phenomenon and still keep the error sufficiently small, the choice $\mu_\Theta = \mu = \pi/4$ seems to be adequate.

The values of K_Θ for case 1 were computed using the (43) where $K_\Theta = \nu_\Theta(\cdot) + q_\Theta$ and $q_\Theta = 2.1k_0^\Theta\mu_\Theta$ with $\mu_\Theta = \pi/4$ and $k_0^\Theta = 1$ resulting in $q_\Theta = 1.649$. Then $\nu_\Theta(\cdot) \ge |F_\Theta(\cdot)| = k_1^\Theta\left|e_2^\Theta\right| + |b(e,\eta)|$, assuming that the error is $\left|e_2^\Theta\right| \approx 0$ leads to $\nu_\Theta(\cdot) \ge |b(e,\eta)|$ (See (55)).

$$\nu_\Theta(\cdot) \ge k_a\left[C_{m_0} + C_{m_\alpha}\eta + C_{m_q}\left(\frac{\bar{c}}{V}\right)\xi_2\right], \tag{55}$$

where $k_a = \frac{\bar{q}S\bar{c}}{I_{yy}}$. Then, using the stability derivatives and properties listed in Table 1, and the boundaries $|\eta| = |\alpha| \le \pi/4$ rad and $|\xi_2| = |q| \le \pi/2$ rad/s we have $\nu_\Theta(\cdot) = 11.776$ and consequently $K_\Theta = 13.425$. To complete the controller (case 1) it is necessary to compute the value of g_2 of (40) $g_2 = k_a C_{m_{\delta_p}}$, with $C_{m_{\delta_p}} = -0.45$ we obtain $g_2 = -36.25$. Finally, the UIR controller is written as in (56).

$$u_\Theta = -g_2^{-1} K_\Theta sat\left(\frac{s_\Theta}{\mu_\Theta}\right)$$

$$= 0.38 \cdot sat\left(\frac{1\sigma_\Theta + 1e_1^\Theta + e_2^\Theta}{\pi/4}\right). \quad (56)$$

For case 2, K_Θ is calculated by means of (48). Considering $\left|e_2^\Theta\right| \approx 0$ again, keeping in mind that $|\theta_1| = \left|Cm_{\delta p}\right| = 0.45$, $\hat{\theta}_1 = 0.5$ and reusing $|b(e,\eta)|$ e q_Θ from previous case, the controller gain is computed as in (57).

$$K_\Theta = \left(\frac{\hat{\theta}_1}{\theta_1} - 1\right)|b(e,\eta)| + q_\Theta\left(\frac{\hat{\theta}_1}{\theta_1}\right),$$
$$K_\Theta = 3.166. \quad (57)$$

With $\hat{a}(\cdot) = g_2 = -k_a\hat{\theta}_1$ and $\hat{F}_\Theta(\cdot) = F_\Theta(\cdot)$ is possible to complete the UIR controller for case 2 which is given by the expression in (58).

$$u_\Theta = \frac{-\hat{F}_\Theta(\cdot) - K_\Theta \cdot sat(s_\Theta/\mu_\Theta)}{\hat{a}(\cdot)} = \frac{-k_1^\Theta e_2^\Theta - b(e,\eta) - K_\Theta \cdot sat(s_\Theta/\mu_\Theta)}{g_2},$$
$$u_\Theta = \frac{-k_1^\Theta e_2^\Theta - b(e,\eta) - 3.166 \cdot sat\left(\frac{1\sigma_\Theta + 1e_1^\Theta + e_2^\Theta}{\pi/4}\right)}{-k_a\hat{\theta}_1}. \quad (58)$$

With $b(e,\eta) = k_a\left[C_{m_0} + C_{m_\alpha}\eta + C_{m_q}\left(\frac{\bar{c}}{V}\right)\left(e_2^\Theta + \Theta'_{ref}\right)\right]$. In order to make the simulations more realistic, an actuator for elevator was modeled as a first order differential equation $\dot{\delta}_p = -20.2\delta_p + 20.2u_\Theta$ with saturation to ensure the maximum elevator deflection $|\delta_p| \leq 30°$ and maximum rate $|\dot{\delta}_p| \leq 720°/s$. The simulation results are shown in Fig. 4.

It can be noted in Fig. 4 that both controllers achieve good performance with tracking errors not higher than 0.1 radians ($< 5.7°$). Controller from case 2 approach proved to be more accurate tracking the reference signal and demanded less control activity. It should be noted that the gains K_Θ for each case are the minimal ones able to guarantee the correct operation of the controllers, therefore, in order to illustrate a possible degradation and/or improvement of tracking error with other gains, the response of the simplified UIR (case 1) was simulated with the gains $\frac{1}{4}K_\Theta$ and $4K_\Theta$. Fig. 5 confirms the efficiency of the minimal gain K_Θ analytically obtained. When compared to $\frac{1}{4}K_\Theta$ it is easy to check a high degradation of the tracking response and using $4K_\Theta$ gain, the response shows a significant reduction of tracking error.

In order to demonstrate the robustness and large region of attraction of the UIR controller, the maximum value of the reference attitude angle doublet was gradually increased up to 80°, the results are shown in Figs. 6 and 7. In Fig. 6 a good tracking performance can be seen for both controllers, either considering a complete knowledge of the model or in the presence of model uncertainties. Fig. 7 illustrates the control demand for both cases, requiring higher control activity in case 2.

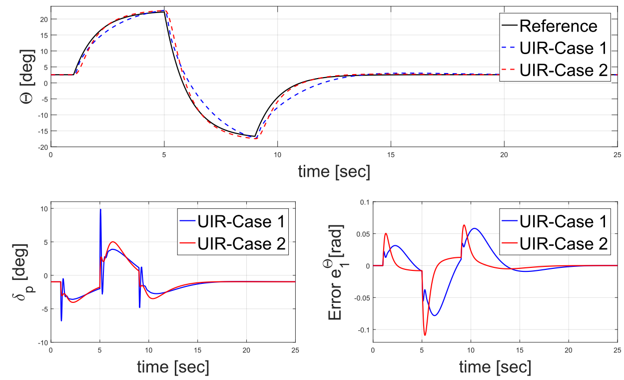

Fig. 4. Attitude tracking using UIR, cases 1 and 2.

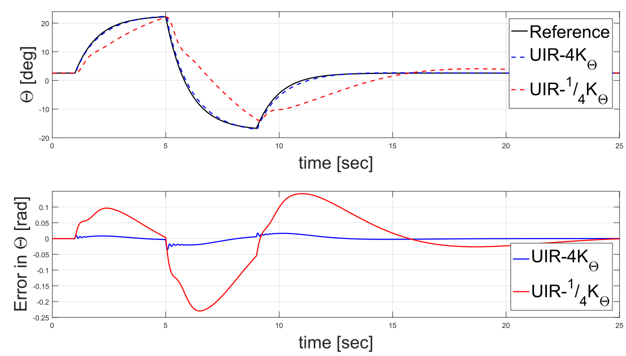

Fig. 5. Attitude tracking using UIR case 1 with $\frac{1}{4}K_\Theta$ and $4K_\Theta$.

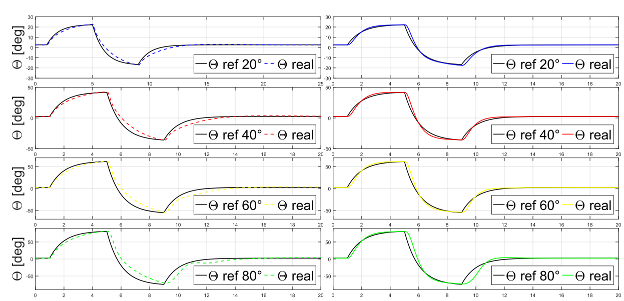

Fig. 6. Attitude tracking for different amplitude references - UIR controller, dashed line (case 1), solid line (case 2).

In this work, two performance indexes are proposed to compare the performance of both studied approaches, a performance index to the accumulated error (AE) defined as $AE = \int_o^t abs(e_1^\Theta)dt$ and one to the Control Demand (CD) as $CD = \int_0^t abs(\delta_p)dt$. Figs. 8 and 9 show less accumulated error to case 2, during the simulation time at expenses of demanding more control activity, this analysis allows to confirm that considering uncertainties in the

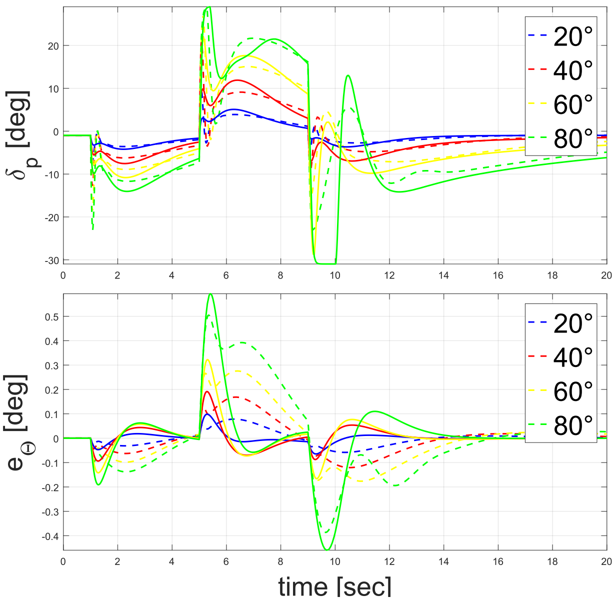

Fig. 7. Control for different amplitude references - UIR controller, dashed line (case 1), solid line (case 2).

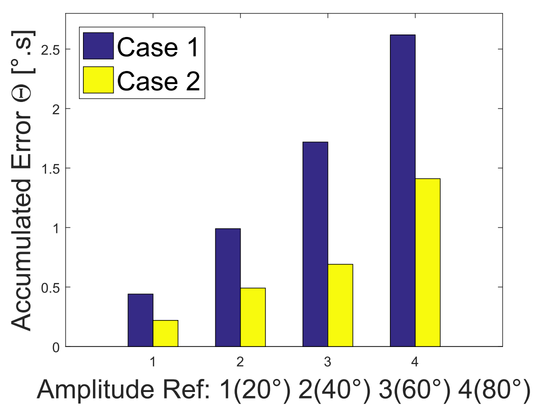

Fig. 8. Comparison between accumulated tracking error, case 1 and 2.

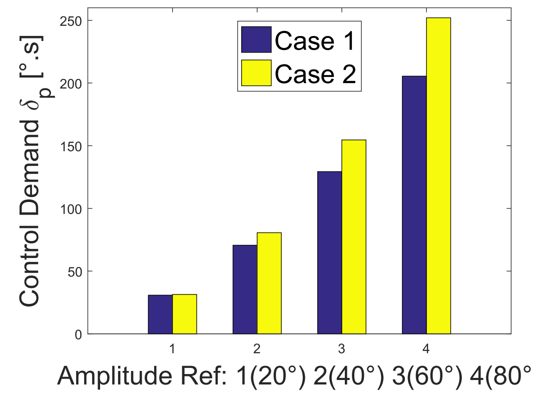

Fig. 9. Comparison between control demand, case 1 and 2.

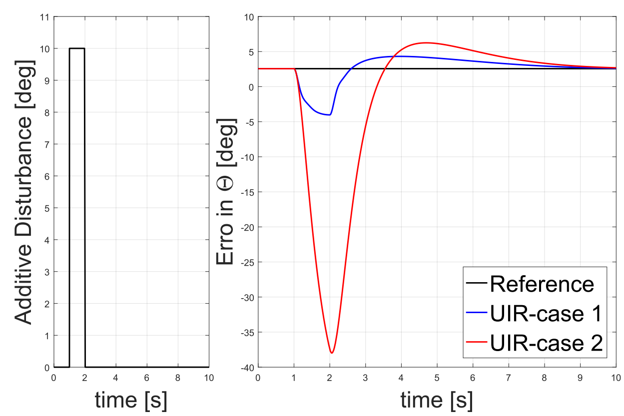

Fig. 10. Disturbance effect of UIR controller, case 1 and 2.

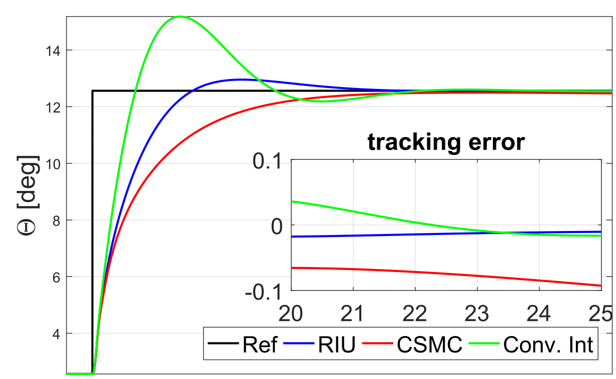

Fig. 11. Response comparison among UIR and previous approaches.

model leads to a more robust controller.

One of the main advantages of the universal integral regulator is the ability to handle disturbances that can cause abrupt system changes. With the UIR controller "on" and flight condition trimmed at V=250 m/s and H=5000 m, an input additive disturbance of 10° was applied to the elevator input between $t = 1s$ and $t = 2s$. In Fig. 10 it is possible to see the additive pulse disturbance shape and the aircraft response for both controllers (cases 1 and 2). The simulation results showed a good behavior of the attitude angle response even in the presence of the disturbance, being the UIR case 1 which revealed a better transient performance with a tracking error lower than 5°.

To finish with this study, the performance of the UIR with CSMC and SMC with conventional integrator $\sigma = \dot{e}_1^{\Theta}$ is compared. As mentioned in the introduction, the UIR is a SMC based technique modified by the introduction of a conditional integrator, this combination has the advantage of improving the transient response caused by the use of a conventional integrator and eliminates the non-zero error problem caused by the CSMC approach. Fig. 11 shows the response of the attitude angle of the aircraft in study to a step-type reference of 10°. Results confirm the advantages previously mentioned. A similar comparison with a simple dynamic system was done in [34].

9. CONCLUSION

In this paper, the relatively novel control technique Universal Integral Regulator (UIR) was applied to the attitude tracking problem of a fighter aircraft. The main feature of this technique is the ability of retaining the transient response of the ideal SMC ensuring zero tracking error. The aircraft dynamic was written in the control input affine-form and transformed to a normal form by constructing a local diffeomorphism. This transformation made a feedback linearization and it was possible to separate the system into an internal and external dynamics. The exponential stability of the internal dynamics was analytically demonstrated and the external dynamics showed to be asymptotically stable through a Lyapunov's direct method stability analysis. It was possible to find a simulation-based methodology to adequately choose the boundary layer of the CSMC and a direct relationship between the boundary layer and the main gain of the controller, which was analytically determined, representing one of the main contributions of this work. The robustness of the control technique was extensively demonstrated through simulations and the system behavior was as expected due to the uncertainties considered in the analytical design. The UIR demonstrated good performance under model uncertainties by the fact that the actuator was implemented (in simulations) but not considered along the design of the controller. The results showed good performance of the UIR to tackle with additive input disturbances and exhibited a fast convergence of the tracking error guaranteeing zero steady-state error without degrading the transient system response. This was done even in the presence of high reference angles and without using any gain scheduling. The comparison between both approaches was done through the proposition of two performance indexes related with the accumulated error and control demand.

REFERENCES

[1] S. A. Salman, A. G. Sreenatha, and J. Y. Choi, "Attitude dynamics identification of unmanned aircraft vehicle," *International Journal of Control Automation and Systems*, vol. 4, no. 6, pp. 782-787, 2006.

[2] E. M. Jafarov and R. Tasaltin, "Robust sliding-mode control for the uncertain mimo aircraft model f-18," *IEEE Transactions on Aerospace and Electronic Systems*, vol. 36, no. 4, pp. 1127-1141, 2000.

[3] H. Vo and S. Seshagiri, "Robust control of f-16 lateral dynamics," *Proc. of IEEE Industrial Electronics Annual Conference*, pp. 343-348, IEEE, 2008.

[4] O. Akyazi, M. A. Usta, and A. S. Akpinar, "A self-tuning fuzzy logic controller for aircraft roll control system," *International Journal of Control Science and Engineering*, vol. 2, no. 6, pp. 181-188, 2012.

[5] V. G. Nair, M. Dileep, and V. George, "Aircraft yaw control system using lqr and fuzzy logic controller," *International Journal of Computer Applications*, vol. 45, no. 9, pp. 25-30, 2012.

[6] G. Sudha and S. N. Deepa, "Optimization for pid control parameters on pitch control of aircraft dynamics based on tuning methods," *Applied Mathematics & Information Sciences*, vol. 10, no. 1, pp. 343-350, 2016.

[7] D. Lee, H. J. Kim, and S. Sastry, "Feedback linearization vs. adaptive sliding mode control for a quadrotor helicopter," *International Journal of Control, Automation and Systems*, vol. 7, no. 3, pp. 419-428, 2009.

[8] J. Hauser, S. Sastry, and G. Meyer, "Nonlinear control design for slightly non-minimum phase systems: Application to v/stol aircraft," *Automatica*, vol. 28, no. 4, pp. 665-679, 1992.

[9] N. Van Chi, "Adaptive feedback linearization control for twin rotor multiple-input multiple-output system," *International Journal of Control, Automation and Systems*, vol. 15, no. 3, pp. 1267-1274, 2017.

[10] Y. Wei, J. Qiu, P. Shi, and M. Chadli, "Fixed-order piecewise-affine output feedback controller for fuzzy-affine-model-based nonlinear systems with time-varying delay," *IEEE Transactions on Circuits and Systems*, vol. 64, no. 4, pp. 945-958, 2017.

[11] R. Rysdyk and A. J. Calise, "Robust nonlinear adaptive flight control for consistent handling qualities," *IEEE Transactions on Control Systems Technology*, vol. 13, no. 6, pp. 896-910, 2005.

[12] Q. Wang and R. F. Stengel, "Robust nonlinear control of a hypersonic aircraft," *Journal of Guidance, Control, and Dynamics*, vol. 23, no. 4, pp. 577-585, 2000.

[13] A. L. Da Silva, "Procedimento de projeto de leis de controle de vôo de aeronaves utilizando o controle à estrutura variável," Master's thesis, Instituto Tecnológico de Aeronáutica, 2007.

[14] H. Xu, M. D. Mirmirani, and P. A. Ioannou, "Adaptive sliding mode control design for a hypersonic flight vehicle," *Journal of Guidance, Control, and Dynamics*, vol. 27, no. 5, pp. 829-838, 2004.

[15] H. Sun, S. Li, and C. Sun, "Finite time integral sliding mode control of hypersonic vehicles," *Nonlinear Dynamics*, vol. 73, no. 1-2, pp. 229-244, 2013.

[16] H. Bouadi, H. Wu, and F. Mora-Camino, "Flight path tracking based-on direct adaptive sliding mode control," *Proc. of IEEE Intelligent Vehicles Symposium*, pp. 25-30, 2011.

[17] I. A. Shkolnikov and Y. B. Shtessel, "Aircraft nonminimum phase control in dynamic sliding manifolds," *Journal of Guidance, Control, and Dynamics*, vol. 24, no. 3, pp. 566-572, 2001.

[18] S. Lim and B. S. Kim, "Aircraft cas design with input saturation using dynamic model inversion," *International Journal of Control, Automation, and Systems*, vol. 1, no. 3, pp. 315-320, 2003.

[19] Y. Wei, J. H. Park, J. Qiu, L. Wu, and H. Y. Jung, "Sliding mode control for semi-markovian jump systems via output feedback," *Automatica*, vol. 81, pp. 133-141, 2017.

[20] W. Qi, G. Zong, and H. R. Karim, "Observer-based adaptive smc for nonlinear uncertain singular semi-markov jump systems with applications to dc motor," *IEEE Transactions on Circuits and Systems*, vol. 65, no. 9, pp. 2951-2960, 2018.

[21] J.-J. E. Slotine and W. Li, *Applied Nonlinear Control*, vol. 199, Prentice hall Englewood Cliffs, New Jersey, 1991.

[22] Q. Khan, A. I. Bhatti, S. Iqbal, and M. Iqbal, "Dynamic integral sliding mode for mimo uncertain nonlinear systems," *International Journal of Control, Automation and Systems*, vol. 9, no. 1, pp. 151-160, 2011.

[23] H. K. Khalil, "Improved performance of universal integral regulators," *Journal of Optimization Theory and Applications*, vol. 115, no. 3, pp. 571-586, 2002.

[24] H. K. Khalil, "Universal integral controllers for minimum-phase nonlinear systems," *IEEE Transactions on Automatic Control*, vol. 45, no. 3, pp. 490-494, 2000.

[25] S. B. Prusty, S. Seshagiri, U. C. Pati, and K. K. Mahapatra, "Sliding mode control of coupled tanks using conditional integrators," *Proc. of IEEE Indian Control Conference*, pp. 146-151, 2016.

[26] A. Benamor, L. Chrifi-Alaui, H. Messaoud, and M. Chaabane, "Sliding mode control, with integrator, for a class of mimo nonlinear systems," *Engineering*, vol. 3, no. 05, pp. 435-444, 2011.

[27] Y. Liu, M. Lu, X. Wei, H. Li, J. Wang, Y. Che, B. Deng, and F. Dong, "Introducing conditional integrator to sliding mode control of dc/dc buck converter," *Proc. of IEEE International Conference on Control and Automation*, pp. 891-896, 2009.

[28] M. Burger, *Disturbance Rejection Using Conditional Integrators: Applications to Path Manoeuvring under Environmental Disturbances for Single Vessels and Vessel Formations*, Master's thesis, Norwegian University of Science and Technology, 2011.

[29] V. C. Nguyen and G. Damm, "Mimo conditional integrator control for unmanned airlaunch," *International Journal of Robust and Nonlinear Control*, vol. 25, no. 3, pp. 394-417, 2015.

[30] S. Seshagiri and E. Promtun, "Sliding mode control of f-16 longitudinal dynamics," *Proc. of IEEE American Control Conference*, pp. 1770-1775, 2008.

[31] E. Promtun and S. Seshagiri, "Sliding mode control of pitch-rate of an f-16 aircraft," *International Journal of Mechanical, Aerospace, Industrial, Mechatronic and Manufacturing Engineering*, vol. 3, no. 9, pp. 1108-1114, 2009.

[32] M. S. de Sousa, P. Paglione, F. L. C. Ribeiro, and R. G. A. da Silva, "Use of universal integral regulator to control the flight dynamics of flexible airplanes," *Proc. of 22nd International Congress of Mechanical Engineering*, COBEM, 2013.

[33] R. B. Campos, S. S. da Cunha Júnior, M. S. de Sousa, N. Santos, and C. da Silva, "Controle de uma aeronave flexível," *Revista Interdisciplinar de Pesquisa em Engenharia*, vol. 2, no. 20, pp. 79-88, 2017.

[34] S. Seshagiri and H. K. Khalil, "Robust output feedback regulation of minimum-phase nonlinear systems using conditional integrators," *Automatica*, vol. 41, no. 1, pp. 43-54, 2005.

[35] M. Sousa, *Projeto de um Sistema de Controle de uma Aeronave de Estabilidade Variável Usando o Método do Modelo de Referência*, Master's thesis, Technological Institute of Aeronautics, Brazil, 2005.

[36] H. K. Khalil, *Nonlinear Systems*, vol. 9, Prentice Hall, New Jersey, 2002.

Yohan Díaz-Méndez received his B.S. degree in Aeronautical Engineering in 2010 from the Universidad Nacional Experimental Politécnica de la Fuerza Armada (Venezuela), an M.S. and Ph.D. degrees in Mechanical Engineering from the Federal University of Itajubá (Brazil), in 2014 and 2018 respectively. He is currently an Adjunct Professor of Mechanical-Aeronautical Engineering at Federal University of Itajubá. His research interests include nonlinear aircraft control, structural damage detection and passive structural vibration control.

Marcelo S. de Sousa received the B.S., M.S. and Ph.D. degrees in Aeronautical Engineering from the Technological Institute of Aeronautics - ITA, (Brazil), in 2001, 2005, and 2013, respectively. He worked at the EMBRAER aircraft manufacturer and currently is an Adjunct Professor of Mechanical-Aeronautical Engineering at Federal University of Itajubá, UNIFEI (Brazil). His research interests include aircraft modeling, simulation and linear and nonlinear control.

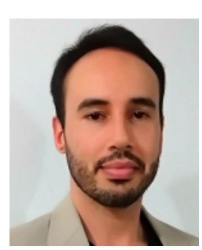

Guilherme Gomes received the B.S., M.S. and Ph.D. degrees in Mechanical Engineering from the Federal University of Itajubá (Brazil), in 2014, 2016, and 2017 respectively. He holds a Master's degree in Mechanical/Industrial Engineering from the École Nationale d'Ingénieurs de Metz (France). He is currently is an Adjunct Professor of Mechanical Engineering at Federal University of Itajubá. His research interests are in mechanical vibrations, structural damage detection, numerical methods, optimization and engineering materials.

Sebastião S. Cunha received the B.S., M.S. and Ph.D. degrees in Mechanical Engineering from the Federal University of Uberlândia (Brazil), in 1996, 1999, and 2004 respectively. He is currently an Associate Professor of Mechanical Engineering at Federal University of Itajubá. His research interests are in mechanical vibrations, mechanical systems design, optimization and control.

Alexandre Ramos received the B.S. in Electronic Engineering from the University of Vale do Paraíba in 1985, his M.S. and Ph.D. degrees in Electronic and Systems Engineering from Aeronautics Institute of Technology (Brazil), in 1992 and 1996, respectively. He holds Postdoctorate's studies in the Ecole Nationale de l'Aviation Civile (France) in 2013-2014. His research interests are in information systems, control of electronic processes and analytical models and simulation.

Publisher's Note Springer Nature remains neutral with regard to jurisdictional claims in published maps and institutional affiliations.